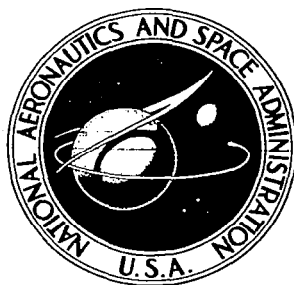


**NASA CONTRACTOR
REPORT**



NASA CR-71

0099410



TECH LIBRARY KAFB, NM

NASA CR-611

**STUDY OF THE EFFECTS OF
A PLASMA IN THE NEAR-ZONE
FIELD OF AN ANTENNA**

by W. C. Taylor

Prepared by

STANFORD RESEARCH INSTITUTE

Menlo Park, Calif.

for Langley Research Center



STUDY OF THE EFFECTS OF A PLASMA IN THE NEAR-ZONE
FIELD OF AN ANTENNA

By W. C. Taylor

Distribution of this report is provided in the interest of
information exchange. Responsibility for the contents
resides in the author or organization that prepared it.

Prepared under Contract No. NAS 1-4973 by
STANFORD RESEARCH INSTITUTE
Menlo Park, Calif.

for Langley Research Center

NATIONAL AERONAUTICS AND SPACE ADMINISTRATION

For sale by the Clearinghouse for Federal Scientific and Technical Information
Springfield, Virginia 22151 - Price \$2.00

ABSTRACT

A program of measurements is reported showing the effects on an antenna caused by a plasma in the near field. The measurements were performed with X-band apertures in ground planes exposed to plasmas in a 12-inch shock tube and in an RF-heated plasma jet.

The effects of plasma on the antenna reflection coefficient were measured in a series of shock-tube firings at two different collision frequencies. In the plasma jet, where the plasma layer over the antenna was thin compared with a wavelength, both reflection coefficient and total impedance were measured.

Patterns were measured in the plasma jet over a large range of electron density. [In addition it was demonstrated that an over-dense plasma layer in the near field reduces the far-field radiation level by at least 10 dB more than the same layer located just outside the near field.]

All these measurements show that the small boundary region near the ground plane, where electron density falls essentially to zero, significantly influences the plasma effects compared with predictions based on a uniform plasma.

CONTENTS

ABSTRACT	11
LIST OF ILLUSTRATIONS	iv
I INTRODUCTION	1
II DESCRIPTION OF FACILITIES AND EQUIPMENT	3
Twelve-Inch Shock Tube	3
RF-Heated Plasma Jet	3
III PLASMA DIAGNOSTIC METHODS	12
Shock-Tube Diagnostics	12
Plasma-Jet Diagnostics	14
IV RESULTS OF ADMITTANCE MEASUREMENTS	16
Reflection Coefficient Measurements	16
Complete Admittance Measurements	19
V RESULTS OF PATTERN AND TRANSMISSION EFFICIENCY MEASUREMENTS	24
Patterns	24
Transmission Efficiency	24
VI CONCLUSIONS AND RECOMMENDATIONS FOR FUTURE WORK	31
REFERENCES	33

ILLUSTRATIONS

Fig. 1	X-Band Antenna Installation in Shock Tube	4
Fig. 2	Illustration of X-Band Antenna, Pattern, Range, and Auxiliary Plasma-Jet Systems	5
Fig. 3	Photograph of Plasma Jet, Showing Flow Over Antenna Face (Center), 14-MHz Tuning and Matching System (Bottom), and Probe Support Rod (Running Vertically Through Center)	7
Fig. 4	Teflon-Filled Slot With Ground Plane	9
Fig. 5	Teflon-Filled Antenna in Plasma Jet With Probe in Plasma Stream	10
Fig. 6	Boron Nitride (BN) Antenna	11
Fig. 7	Electron Density Profiles Inferred from Ion Current Measurements: (1) Shock Tube, 0.1 torr Initial Pressure; (2) Plasma Jet With Narrow Quartz Tube (a) Against Antenna Face and (b) $\sim \lambda_0/2$ Away; (3) Plasma Jet With Wide Quartz Tube Against Face for Two Argon Flow Rates	13
Fig. 8	Double-Probe Current Characteristic Taken in Plasma Jet With Simultaneous Triangular-Wave Driving Voltage	15
Fig. 9	Simultaneous Recording of Ion Probe Current (top trace) and Reflected X-Band Signal During a Shock Tube Firing	16
Fig. 10	Reflection Coefficient Measurements of Open Waveguide Compared With Theory	17
Fig. 11	Reflection Coefficient Measured in Shock Tube Installation as a Function of Thickness of Mylar Separating Metal Reflector and Ground Plane	18
Fig. 12	Reflection Coefficient Data from Shock Tube (1.0 torr) Compared With Theory	20

ILLUSTRATIONS (Concluded)

Fig. 13	Reflection Coefficient of Teflon and BN Antennas in Plasma Jet Compared With Plasma Phase Constant β/β_0	21
Fig. 14	Measured Normalized Admittance of Open Waveguide Terminated With Ground Plane in Plasma Jet, Compared With Theory for Uniform Plasma	22
Fig. 15	Patterns of Teflon-Filled Slot Compared With Free Space (Profiles Similar to 2a)	25
Fig. 16	Patterns of Teflon Slot	26
Fig. 17	Patterns Made With Thickest Electron Density Profiles	27
Fig. 18	Measured Broadside Attenuation Compared With Plane-Wave Theory	29
Fig. 19	Plot of Signal Received by 5-mm Dipole Probe Versus Distance on Axis	30

I INTRODUCTION

This report covers the second one-year study program by Stanford Research Institute (SRI) dealing with the effects of a plasma in the near-zone field of an antenna. Of particular interest are (1) the ability to deduce properties of the plasma by terminal impedance measurements on the antenna, and (2) the ability of the antenna to radiate in the presence of a plasma in its near field. A concurrent study of DC probe diagnostics is now in progress in this laboratory.* These problems are being studied in re-entry flight test programs. These programs are being carried out in conjunction with the Re-entry Attenuation Measurement (RAM) Project of NASA-Langley Research Center.

One of the attributes of diagnostics by flush-mounted RF apertures is that the fields do not perturb the plasma. However, the accuracy in determining the plasma properties by terminal impedance measurements has been questioned in the past for two reasons:

- (1) The impedance model used for interpreting the measurements is considered inadequate; and
- (2) The spatial resolution "cell" is the entire near-field region. The effects of any nonuniformity in the plasma in this region will be integrated in the terminal impedance measurement.

The first year of the program^{1†} was devoted largely to small loops and dipoles. It was shown both experimentally and theoretically that because of ohmic dissipation in the plasma by currents associated with near fields, only a fraction of the power delivered by loops and dipoles to the surrounding media is radiated into a propagating wave. It was found that this fraction has a minimum value at plasma electron resonance, but the effect is usually overwhelmed by the conventional attenuation of the propagating wave when plasma density exceeds critical.

* SRI Project 5771 under contract NAS1-4872

† Numbered references appear at end of text.

The emphasis of the second-year program reported here has been on measurements with radiating rectangular apertures with at least one dimension of the same order as the wavelength. Such aperture antennas are typical of those used for RF diagnostics of plasmas. A program of impedance measurements was initiated as a companion to a concurrent theoretical program at NASA-Langley Research Center. In addition, since the larger radiators generally have more directivity than the small antennas, the effect of the plasma upon the pattern becomes important in evaluating such antennas for transmitting. A series of tests was initiated with emphasis upon possible transmission parallel to the ground plane between the metal and plasma.

The measurements in the earlier program with loops and dipoles were made in seeded hydrocarbon flames at L-band frequencies such that the ratio of collision frequency, ν , to angular microwave frequency, ω , was of the order of unity. The new measurements reported here were made at X-band frequencies in two different facilities, a 12-inch arc-driven shock tube and an RF-heated plasma jet. They were operated in pressure regimes such that ν/ω varies between 10^{-3} and 4×10^{-1} , giving more reactive plasmas than is possible in the flames.

Section II is a short description of these facilities and the equipment used in them for the primary measurements. Section III describes the diagnostic measurements made in both facilities. Sections IV and V present the results of the measurements of impedance, and of patterns and transmission efficiency, respectively.

The author is grateful to T. Morita, W. E. Scharfman and J. B. Chown of SRI and to W. F. Croswell of NASA Langley Research Center for many helpful discussions and suggestions. The measurements were capably performed by R. J. Mora and J. W. Granville.

II DESCRIPTION OF FACILITIES AND EQUIPMENT

Twelve-Inch Shock Tube

Reflection coefficient measurements of an open X-band waveguide terminated in a ground plane were made in an arc-driven shock tube with a 12-inch test section. The tube is patterned after the Camm and Rose² tube, and its performance capabilities are reported in detail in Reference 3. The tube is capable of producing shocks with electron density several orders of magnitude above and below the critical level for X-band frequencies. Figure 1 is a photograph of the installation in the shock tube for some of the earlier measurements. The ground plane was placed parallel to the flow, and the leading edge was made sharp in order to minimize the effects on the flow. The free-stream electron density was inferred from wire probes collecting saturation ion current. The reflection coefficient was measured by monitoring the calibrated output of a directional coupler sampling the reflected power. Both the reflected signal and ion current were displayed as single-sweep oscilloscope traces. The most satisfactory measurements were made when the arrangement shown in Fig. 1 was altered such that the probe was immediately downstream of the aperture and the long aperture dimension was re-installed parallel to the flow in the tube. Two series of measurements were made, one with an initial pressure of 0.1 torr and the other, 1.0 torr. For the low-pressure shots, the aperture was covered with 0.003-inch thick Mylar tape to give a discrete boundary between the plasma outside and air inside. For the higher-pressure shots, the tape required support by a block of polyfoam fixed inside the waveguide.

RF-Heated Plasma Jet

Impedance, transmission, and pattern measurements were made in the electrodeless plasma jet (Fig. 2). Three different X-band antennas were exposed to the stream of low-pressure argon that is heated and ionized

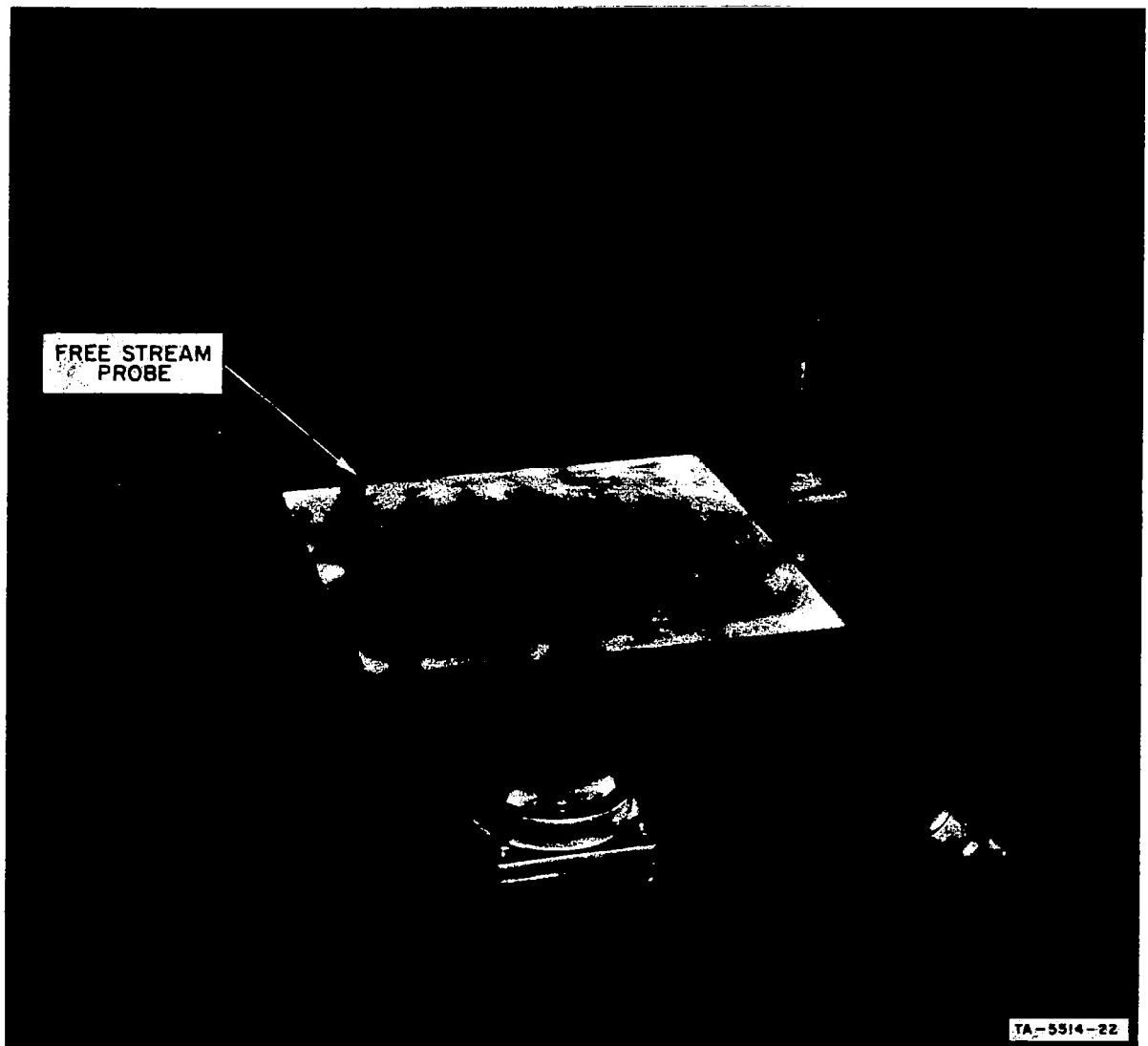
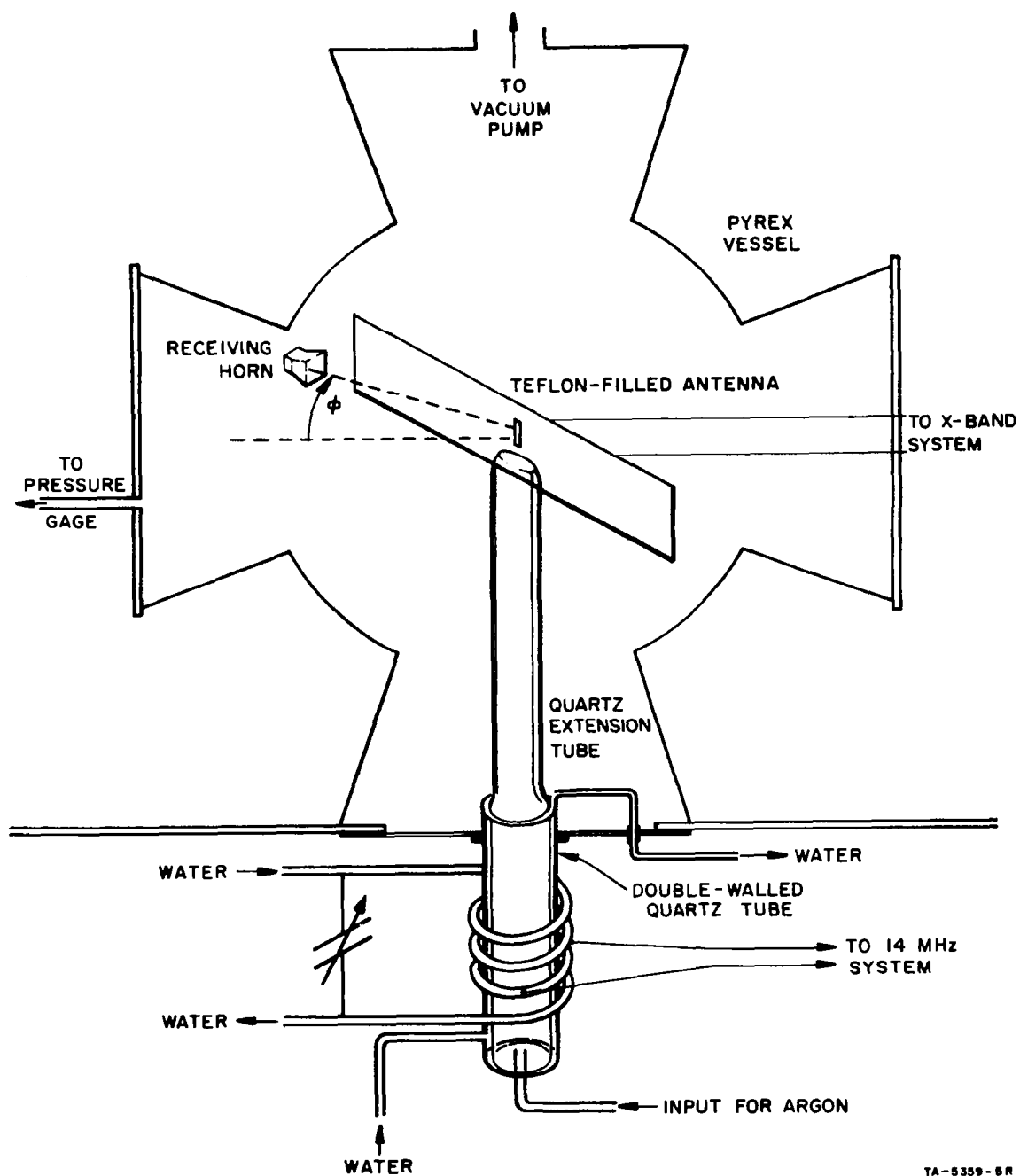


FIG. 1 X-BAND ANTENNA INSTALLATION IN SHOCK TUBE



TA-5359-5R

FIG. 2 ILLUSTRATION OF X-BAND ANTENNA, PATTERN, RANGE, AND AUXILIARY PLASMA-JET SYSTEMS

essentially by a combination of the conventional glow discharge and induction, or ring, discharge. The argon is introduced through a water-cooled quartz tube which is inside a five-turn solenoid portion of an LC tank circuit resonant at 14.6 MHz. A glow discharge is produced by moderate power (< 100 watts) delivered to the circuit via coaxial transmission lines from a radio transmitter capable of delivering up to 15 kW of power. This discharge produces sufficient ionization that when higher power is delivered to the circuit, the RF magnetic field of the solenoid induces in the conducting gas RF currents that are great enough to produce ohmic heating and further ionization of the gas. Both electron density and electron temperature are higher than equilibrium with the gas temperature when argon is used.

The stream was directed by a quartz extension tube with an oval opening toward the antenna near the center of the large Pyrex vessel. The shaped plasma slab extended about 4 cm on each side of the aperture. The electron density along the propagation axis ($\phi = 0^\circ$) is nonuniform in a manner similar to boundary layers on re-entry vehicles, exhibiting a simple maximum at various distances from the ground plane. Some profiles are shown in Section III. The electron density in the stream above the mouth of the extension tube falls typically by a factor of 1/2 in the first 7 cm above the mouth. A convenient control of electron density levels passing over the aperture was achieved by varying the flow velocity of the argon introduced into the plasma generator. For a given amount of RF power delivered to the generator, a range of electron density of about one order of magnitude could be realized by this technique. In all these measurements, the static pressure in the vessel was maintained at 0.5 to 0.7 torr by the Roots-blower booster pump with a 1150-CFM capacity. The diagnostics with double- and single-wire probes are discussed in Section III. Figure 3 is a photograph of the plasma jet used for a prior experiment with an L-band antenna located well below the center of the Pyrex chamber.

The open waveguide terminated with a ground plane was used in this facility. A 0.014-inch thick Mylar sheet covered the entire plane. In addition, two dielectric-loaded slot antennas with ground plane

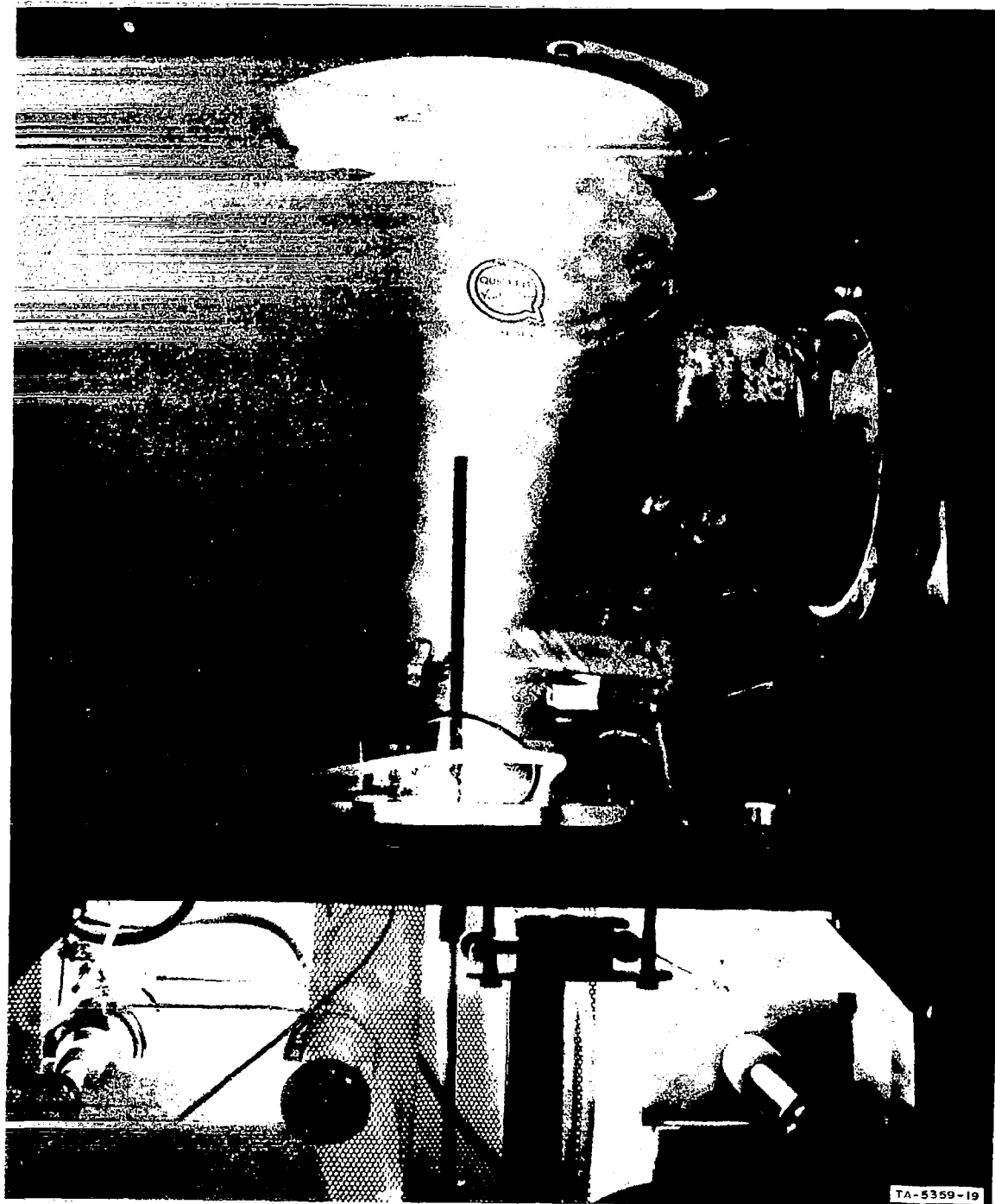
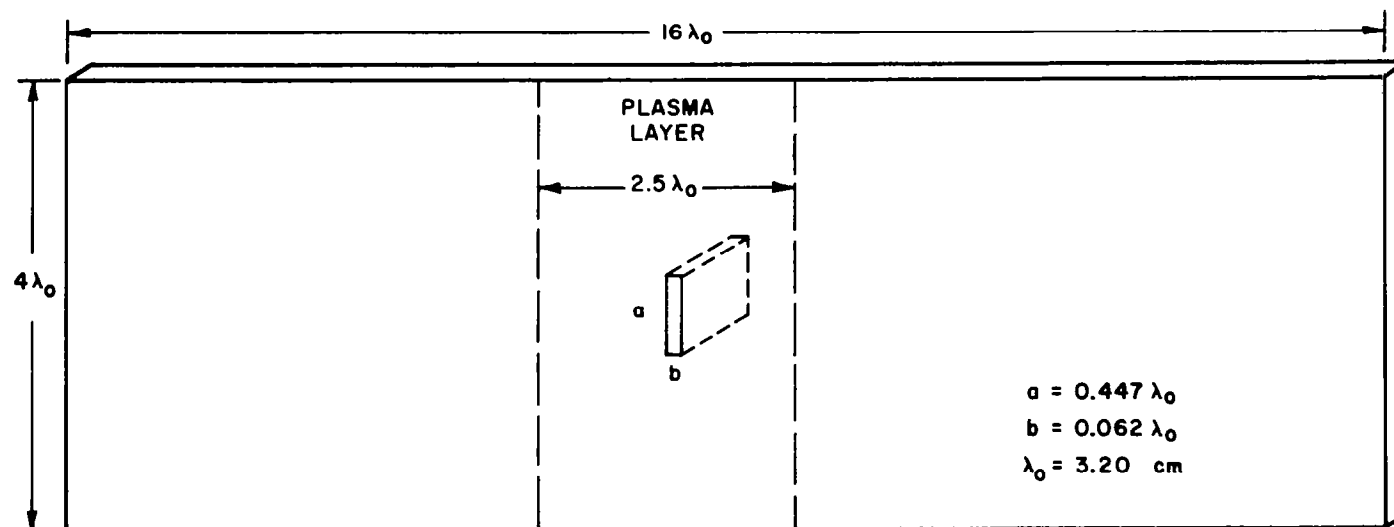


FIG. 3 PHOTOGRAPH OF PLASMA JET, SHOWING FLOW OVER ANTENNA FACE (Center), 14-MHz TUNING AND MATCHING SYSTEM (Bottom), AND PROBE SUPPORT ROD (Running Vertically Through Center)

were used in the plasma jet. One is a radiating section of waveguide filled with Teflon (Fig. 4). The larger waveguide dimension was reduced commensurate with the dielectric constant of Teflon, and the dimension parallel to the E-plane was reduced to 2 mm to encourage high near fields around the aperture. The pattern studies were made in the E-plane of this antenna. Figure 5 is a photograph of this antenna with both plasma and ion probe over the small aperture.

The third antenna used was a section of standard X-band waveguide radiating through a half-wave window made of boron nitride (BN), terminated with a metal ground plane (Fig. 6). The measurements were made at 9.375 GHz with the two dielectric-loaded antennas, and at 10.0 GHz with the open waveguide.

The impedance measurements were made using a standard X-band slotted line. For standing wave ratios $\gtrsim 8$, the ratios were not measured directly, but were computed from the measured 3 dB-width at the minima. The pattern and transmission measurements utilized a small receiving horn nine inches from the aperture as illustrated in Fig. 2. The use of tunnel diode detectors for the thousand-cycle-modulated X-band signal followed by low-pass filters allowed a 40 dB dynamic range above noise for the pattern and transmission measurements despite the presence of strong 14 MHz fields throughout the room.



TA-5514-19

FIG. 4 TEFLON-FILLED SLOT WITH GROUND PLANE

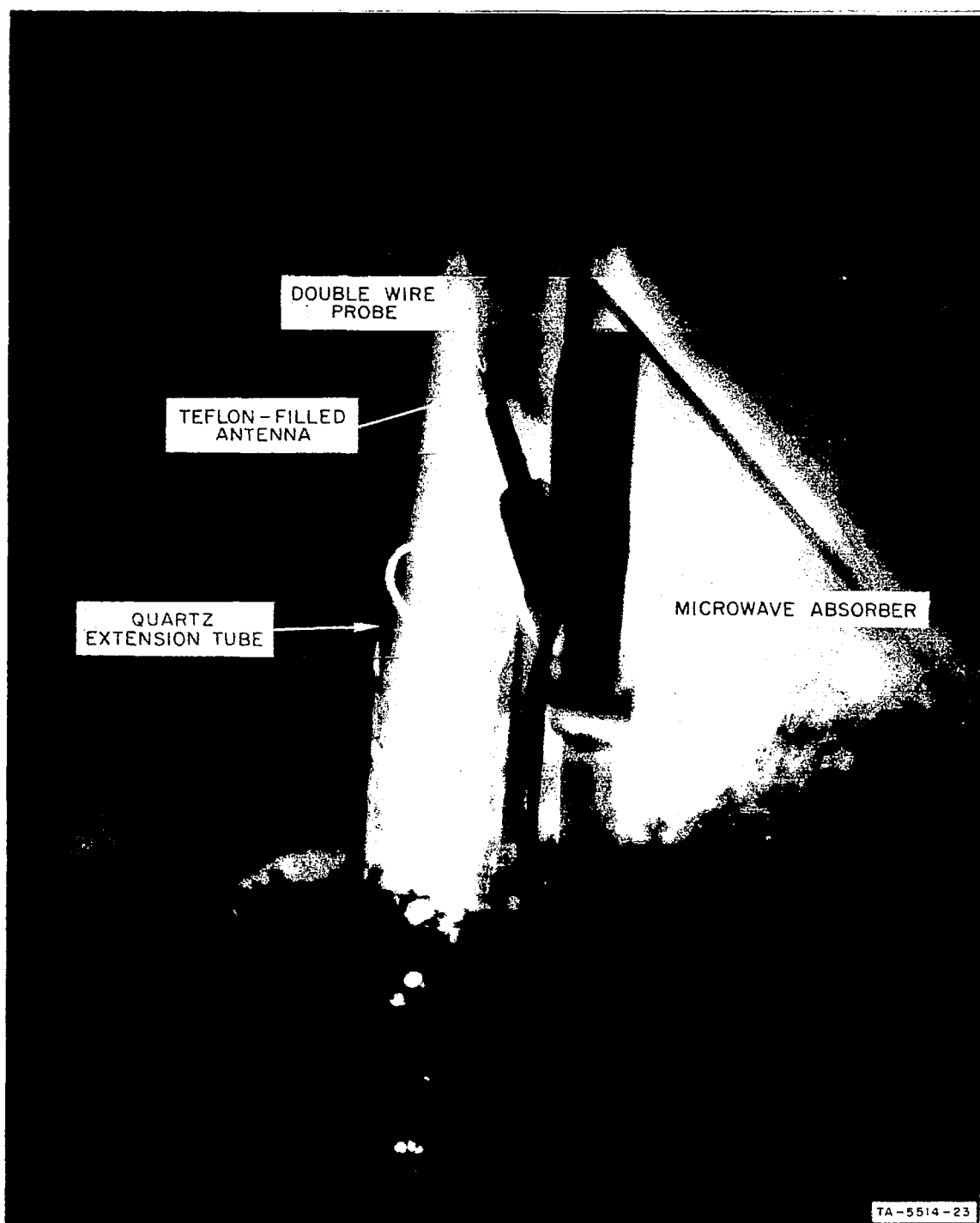


FIG. 5 TEFLON-FILLED ANTENNA IN PLASMA JET WITH PROBE IN PLASMA STREAM

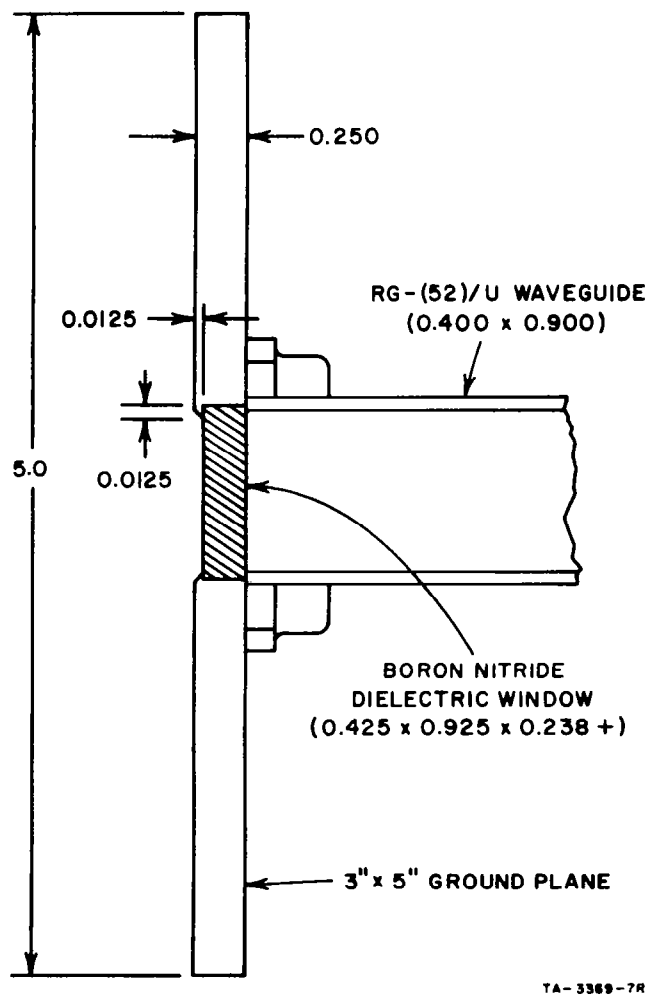


FIG. 6 BORON NITRIDE (BN) ANTENNA

III PLASMA DIAGNOSTIC METHODS

Shock-Tube Diagnostics

The free-stream electron density in the 0.1 torr shock-tube firings was inferred from saturation ion current collected by wire probes of 0.01-inches diameter placed perpendicular to the tube flow. The ion current is free-molecular but is dominated by the directed flow of the tube under these conditions. The relationship between the electron density and the collected current is not linear because of the ion sheath, and is discussed in detail in Ref. 4. This method of determining electron density has been cross-checked by RF interferometer measurements in the range of interest for these shots and was found to agree within 30%. The same method was used with 0.002-inch diameter wires for the 1.0 torr shots with less consistent success from shot to shot. The accuracy under these conditions has not been checked by RF techniques, although the levels inferred have generally agreed with the equilibrium density predicted on the basis of the locally-measured shock velocity and initial pressure.

The average electron collision frequency was calculated from gas-dynamic charts giving the equilibrium density and temperature of the air behind the shock corresponding to the measured initial pressure and shock velocity. This method is considered accurate to within 20%.

A study of the shock-tube boundary layer electron density over a flat plate was made for various levels by Bredfeldt.⁵ One set of measurements was made under conditions pertinent to the 0.1-torr shots in the neighborhood of 10^{12} electrons/cm³. The measured profile is shown in Fig. 7 (profile 1). Since the boundary layer thickness varies as the square root of the distance from the leading edge, the profile shown in Fig. 7 was adjusted slightly to account for the difference between the distance in the initial measurement and that for our application. It would be expected that the profile shown would be

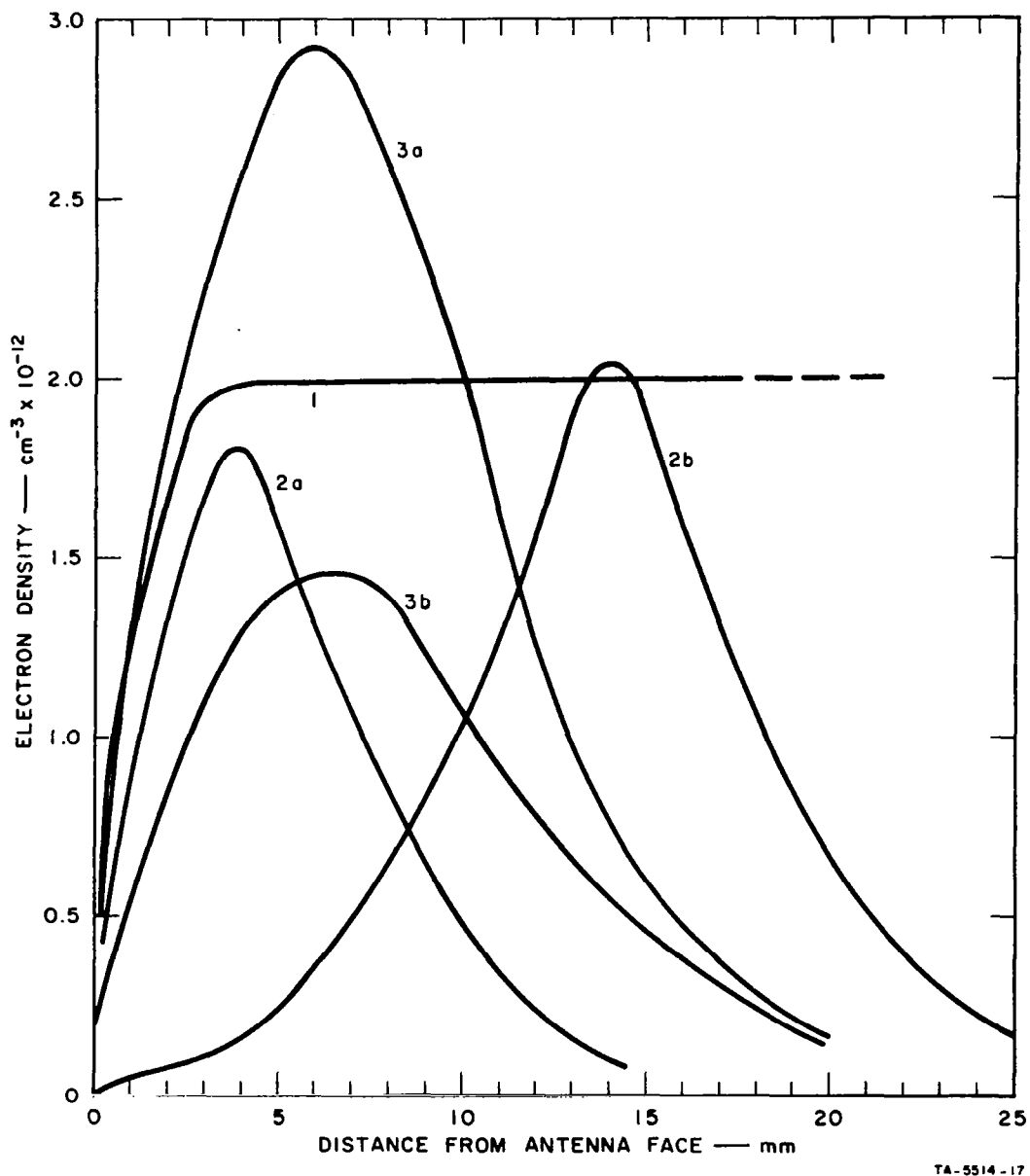


FIG. 7 ELECTRON DENSITY PROFILES INFERRED FROM ION CURRENT MEASUREMENTS: (1) Shock Tube, 0.1 torr Initial Pressure; (2) Plasma Jet With Narrow Quartz Tube (a) Against Antenna Face and (b) $\sim \lambda_0/2$ Away; (3) Plasma Jet With Wide Quartz Tube Against Face for Two Argon Flow Rates

scaled down by a factor of about three for the 1.0-torr shots, although there are no measurements to corroborate this.

Plasma-Jet Diagnostics

Ion current measurements were made with a pair of 0.01- x 0.25-inch iridium wire probes supported, as photographed in Fig. 5, such that elevation and azimuth angle could be varied using a horizontal arm fixed for a given set of measurements. Since the only important gradients in electron density near the aperture were those perpendicular to the ground plane, the only profiles measured regularly were along this direction, taken directly in front of the aperture center.

Saturation ion current was attained by using a 15-volt bias between the two wires. Corrections were made on the basis of Hok's theory⁶ for the fact that the ions are collected over the larger area of the ion sheath than that of the wire probe, and the subsonic flow was low enough to have a negligible effect on ion collection. Originally, estimates of the electron temperature around 2000°K in the argon were used. However, it became apparent, from the RF effects observed in the inferred range of 10^{11} elec/cm³ and below, that the electron density must be higher than calculated by the assumed temperature. Instrumentation was then put to use to measure the full double-probe characteristic, and it was found that, depending upon the flow velocity and input HF power, the electron temperature in front of the aperture varied typically between 500° and 1500°K. When these values were used in connection with the sheath correction, the original lower values of electron density were found to be too low by as much as a factor of three. The circuitry used for the double probes was similar to that of Scharfman⁷ except that a triangular-wave generator was used for sweeping. Figure 8 is a photograph of sample data.

The width of the oval mouth of the quartz extension tube was an important parameter in the experiments. Several different widths were used, ranging from about 0.6 cm to 2.0 cm. The profiles shown in Fig. 7 show that, for a given density at the profile maximum, the narrower tube

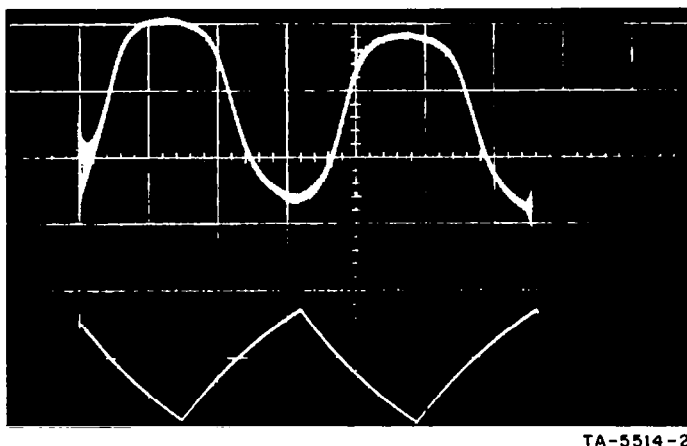


FIG. 8 DOUBLE-PROBE CURRENT CHARACTERISTIC
TAKEN IN PLASMA JET WITH SIMULTANEOUS
TRIANGULAR-WAVE DRIVING VOLTAGE

mouth gives a steeper gradient in electron density, putting the maximum closer to the aperture when the quartz was placed directly against the face of the antenna.

The collision frequency in the plasma jet was estimated by first estimating the argon temperature profile, and from that and the static pressure deducing the argon density profile, hence collision frequency. The estimates for our conditions vary between $3 \times$ and $6 \times 10^{-3} \omega$, depending also upon the power and argon flow velocity. However, a factor of two variation in ν/ω is undiscernible in most plasma effects on microwaves when $\nu/\omega < 10^{-1}$.

It is interesting that, despite the large gradients in electron density perpendicular to the ground plane, the electron temperature was found to be perfectly constant along this axis within the limits of error of the double-probe measurement -- about 10% for this range. Such measurements are consistent with the theory of very efficient thermal transfer within the electron gas.

IV RESULTS OF ADMITTANCE MEASUREMENTS

Reflection Coefficient Measurements

Figure 9 is a photograph of some of the raw data taken in the shock-tube reflection coefficient tests. Although the two traces represent a continuum of values over a considerable range, discrete pairs of corresponding points were chosen at regular intervals for transforming the raw data into instantaneous, matching values of voltage reflection coefficient, $|\Gamma|$, and $(\omega_p/\omega)^2$, where ω_p is the angular electron plasma frequency. The results of this and four other firings at 0.1 torr initial pressure are plotted in Fig. 10. The solid line is the prediction by the Compton theory⁸ for a uniform semi-infinite plasma over the aperture, corresponding to the measured collision frequency

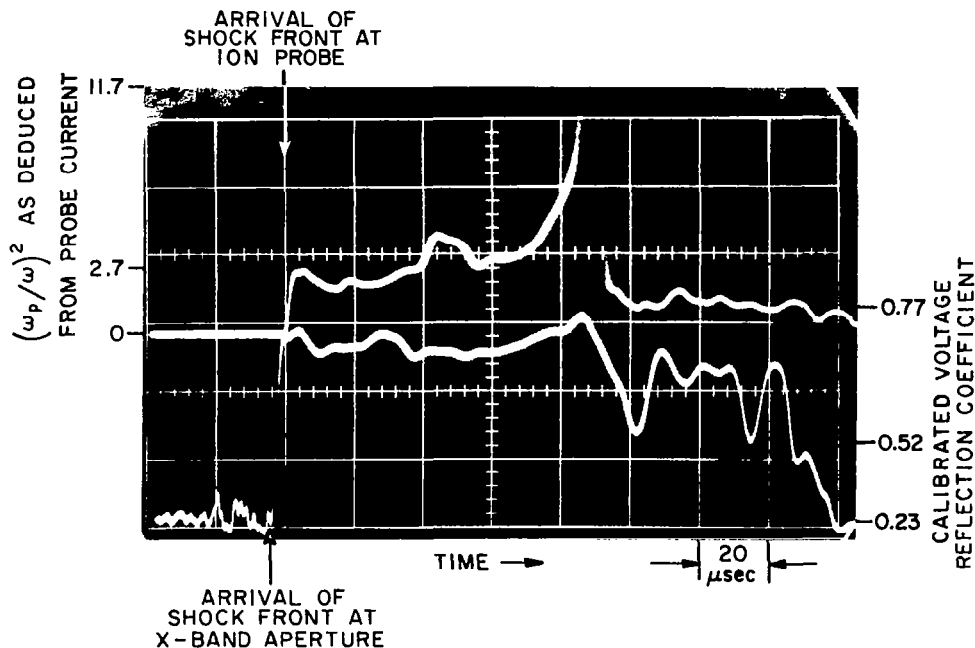
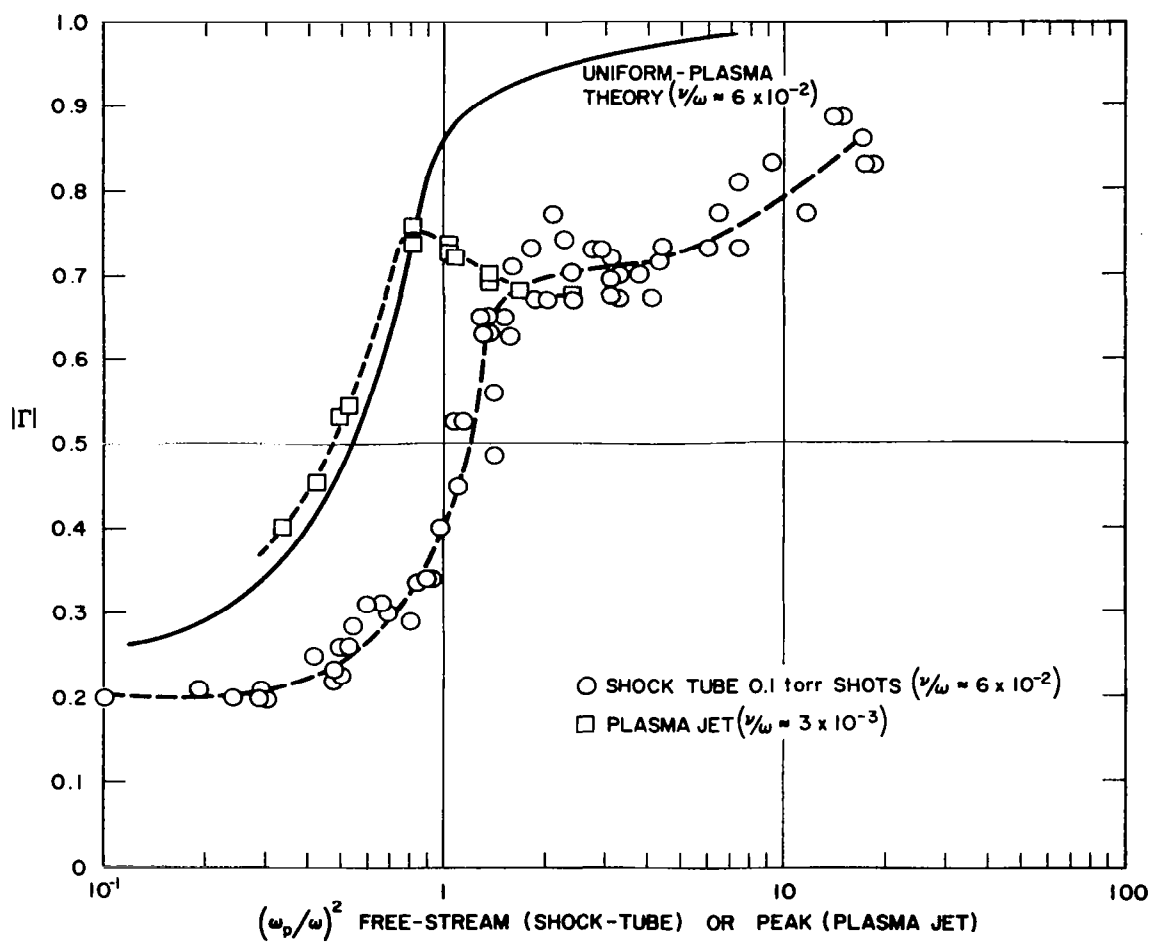


FIG. 9 SIMULTANEOUS RECORDING OF ION PROBE CURRENT (top trace) AND REFLECTED X-BAND SIGNAL DURING A SHOCK TUBE FIRING



TC-5514-2R

FIG. 10 REFLECTION COEFFICIENT MEASUREMENTS OF OPEN WAVEGUIDE COMPARED WITH THEORY

ratio, $v/\omega = 6 \times 10^{-2}$. Although according to Sec. III the error in determining $(\omega_p/\omega)^2$ may be as great as 30%, the small scatter in the data shown in Fig. 10 indicates that if the error is indeed this large it must be systematic rather than random from point to point or shot to shot. However, it appears that more than a 30% horizontal shift is required to reconcile the experimental and theoretical results.

The observation that the reflection coefficient is a sensitive function of small nonuniformities near the aperture appears confirmed by the measurements in the plasma jet. The reflection coefficient of the Teflon antenna at, for example, $(\omega_p/\omega)^2 = 2$ varied between 0.70, when the maximum in the profile was about 6 cm from the face, and 0.86, when the maximum was only 4 cm from the face. Similarly, a metal reflector placed only fractions of wavelengths from the antenna face can effect only limited reflection coefficients, as shown in Fig. 11. The consistency of these results is probably attributable to leaking of radiation through the narrow "boundary" layers. The measured points from the shock-tube tests were corrected for the losses in the guide evidenced by the 0.94 reflection coefficient in Fig. 11 for $t = 0$ (shorted aperture).

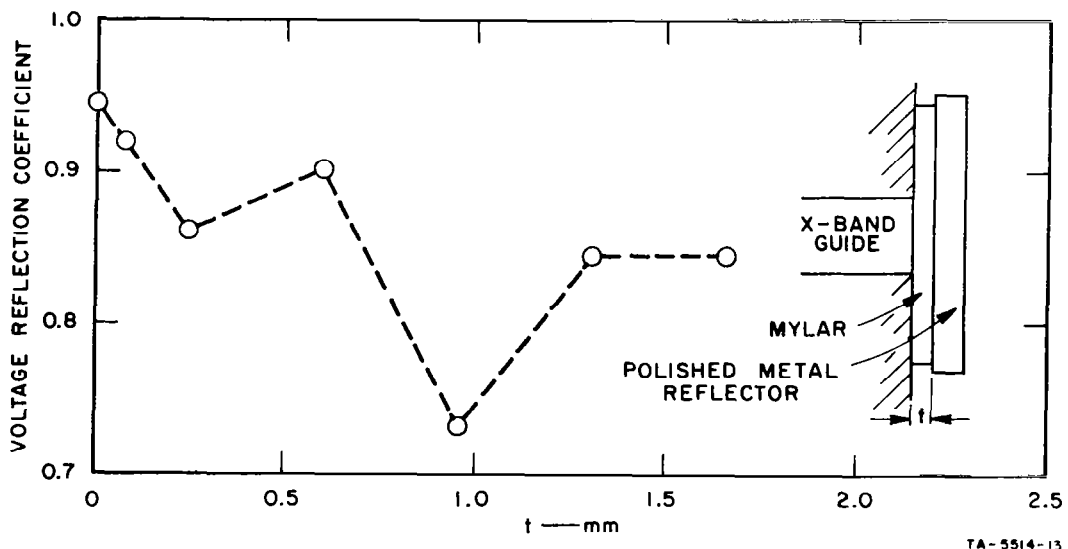


FIG. 11 REFLECTION COEFFICIENT MEASURED IN SHOCK TUBE INSTALLATION AS A FUNCTION OF THICKNESS OF MYLAR SEPARATING METAL REFLECTOR AND GROUND PLANE

Also shown in Fig. 10 are the results of the reflection coefficient measurements with the open waveguide in the plasma jet with profiles similar to 3a and 3b in Fig. 7. Although the collision frequency is lower in this facility, little effect is expected for these differences when $\nu/\omega < 10$. However, significant, unexplained differences are obvious in the results. Although the plasma jet provides a less uniform plasma than the shock tube, the reflection coefficient appears more sensitive to given values of electron density at the profile maximum than to corresponding free-stream values in the shock tube.

Because of the great sensitivity to boundary layer thickness shown in these measurements, and in light of the boundary-layer profile shown in Fig. 7 for the shock tube, it appears that a theory for the nonuniform plasma layer will be necessary for comparison with the measured results in Fig. 10.

The results of the 1.0-torr shots in the shock tube are shown in Fig. 12. It was expected that, since the boundary-layer profile would be scaled down by a factor of three, these shots would agree better with the corresponding theory. This appears to be the case only in the region $0.4 < (\omega_p/\omega)^2 < 2$. Above this region, the same "saturation" effect appears to obtain as in the lower-pressure shots. Inexplicably, the data scatter is greater for these shots than at 0.1 torr.

Figure 13 shows some of the plasma jet reflection coefficient measurements with the other two antennas confronted with plasma profiles similar to 2a in Fig. 7. Figure 7 also shows how the normalized plasma phase constant β/β_0 , varies with $(\omega_p/\omega)^2$ since β/β_0 is identical to the plane-wave conductance of the plasma (normalized to free-space admittance, 377^{-1} mhos). In view of this variation, it is reasonable to expect the observed impedance changes to start around $(\omega_p/\omega)^2 \approx 10^{-1}$.

Complete Admittance Measurements

Five of the reflection coefficient points in Fig. 10 from the plasma-jet tests on the open waveguide are companions to the complete admittance data for five values of $(\omega_p/\omega)^2$ shown in Fig. 14. For

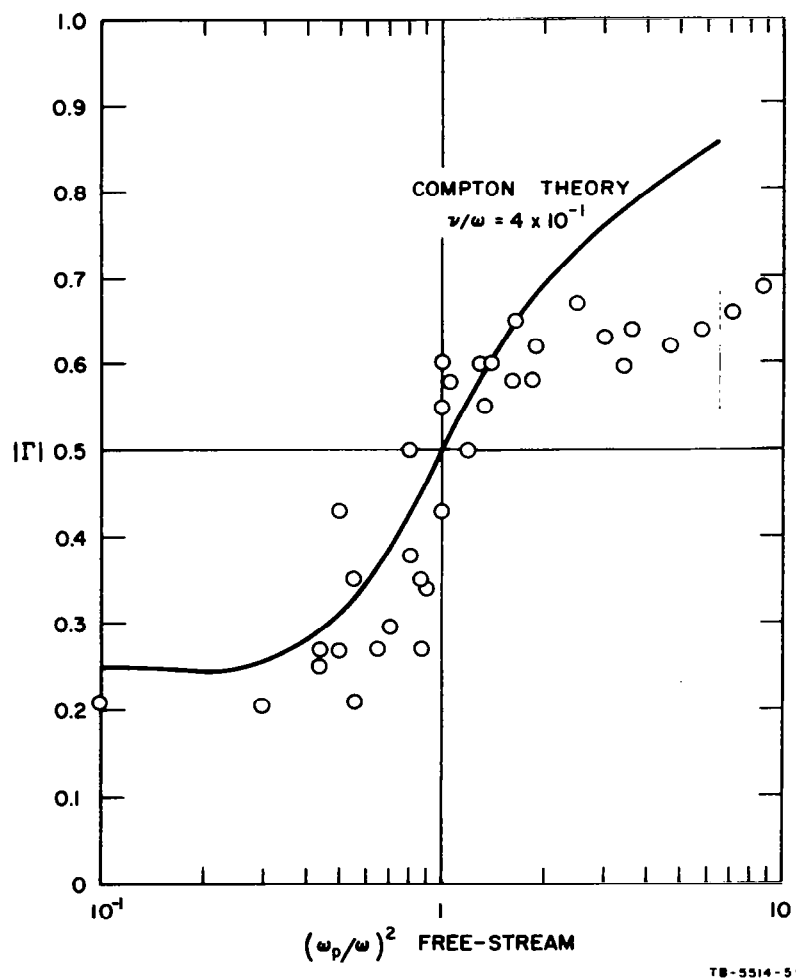
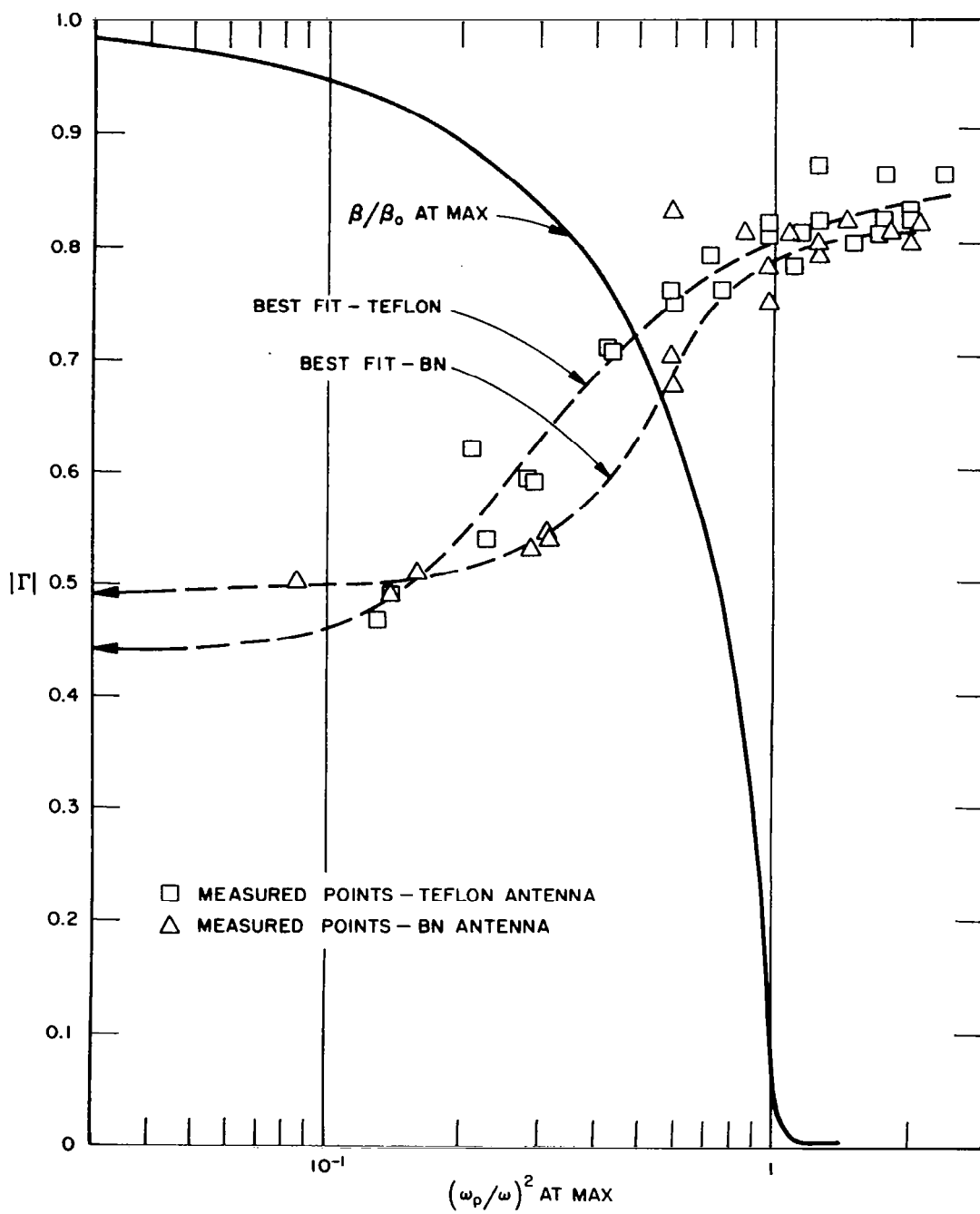


FIG. 12 REFLECTION COEFFICIENT DATA FROM SHOCK TUBE (1.0 torr) COMPARED WITH THEORY



TB-5514-10

FIG. 13 REFLECTION COEFFICIENT OF TEFLON AND BN ANTENNAS ON PLASMA JET COMPARED WITH PLASMA PHASE CONSTANT β/β_0

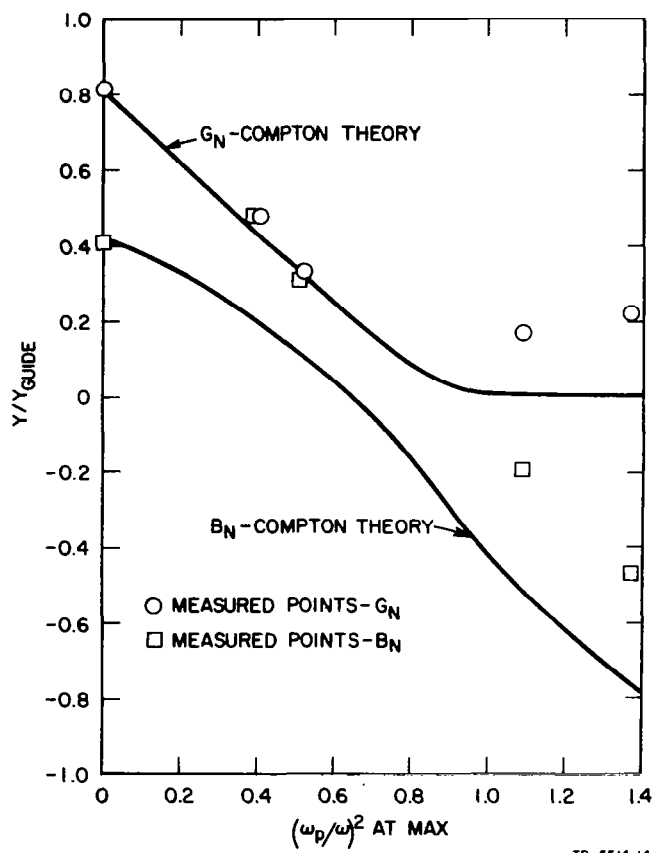


FIG. 14 MEASURED NORMALIZED ADMITTANCE OF OPEN WAVEGUIDE TERMINATED WITH GROUND PLANE IN PLASMA JET, COMPARED WITH THEORY FOR UNIFORM PLASMA

low collision frequency plasmas, where the plasma conductance approaches zero around critical, the most important antenna admittance component in determining reflection coefficient is the conductance. It is seen in Fig. 14 that there is considerable discrepancy between the measured conductance and the uniform-plasma theory in the region around critical. These values are consistent with the low reflection coefficients found in both plasma jet and shock tube for $(\omega_p/\omega) \gtrsim 1$. It is expected that a theory for nonuniform plasma with surface-wave contributions included will improve the agreement.

These five data points were taken with profiles similar to 3a and 3b in Fig. 7. It is expected that the higher VSWR measurements made with the thinner profiles correspond to values of the antenna conductance closer to the theory.

The crossing from capacitive to inductive susceptance for the slot is seen (Fig. 7) by interpolation between the measured points to occur at a value of $(\omega_p/\omega)^2$ about 25% higher than the theoretically predicted value. The discrepancies between experiment and theory for both components of admittance are much smaller, but in the same direction as the discrepancies found by Meltz, Freyheit and Lustig⁹ between theory and experiment for a radial-waveguide-fed gap in a conducting cylinder. Their theory did not take into account the interposition of the glass wall of their plasma vessel between the aperture and the plasma.

V RESULTS OF PATTERN AND TRANSMISSION EFFICIENCY MEASUREMENTS

Patterns

The patterns shown in Fig. 15 were made with a narrow-mouth quartz extension tube that gave slightly narrower profile than the narrowest (2a) shown in Fig. 7. According to Snell's law, a uniform infinite slab of dielectric with index of refraction, n , less than unity will focus rays from a source in it or behind it such that, beyond the slab, no rays will fall at angles greater than a critical angle, $\phi_c = \sin^{-1}n$. The gross features of the two patterns with plasma (Fig. 15) show a marked reduction in signal beyond approximately the angle $\phi_c = \sin^{-1}(\beta_{\max}/\beta_o)$, since the real part of the index of refraction of a plasma is just β/β_o .

However, when the patterns were measured with thicker plasmas with gentler gradients (Fig. 16), this feature began to fill in, and for the thickest plasma used (Fig. 17), this feature is not discernible at all. Apparently, because of the lower gradients in the thicker profiles, the plasma acts less and less like a uniform slab. In addition, the considerable power escaping between plasma and ground plane for the thicker profiles tends to fill in the void as it radiates beyond the limited lateral extent of the plasma slab. Here, again, a close comparison between experiment and a theory will require analysis that recognizes the nonuniformity and finite size of the plasma.

The finer features of the measured patterns are felt to be inconsequential because of the reflections in a container of this kind. The pattern levels were compensated for the impedance mismatch.

Transmission Efficiency

The dashed pattern and the bottom pattern in Fig. 16 were taken under the same plasma conditions (electron density at max = 1.2 times critical) except for the location of the plasma as determined by moving the quartz extension tube away from the antenna face. For the solid

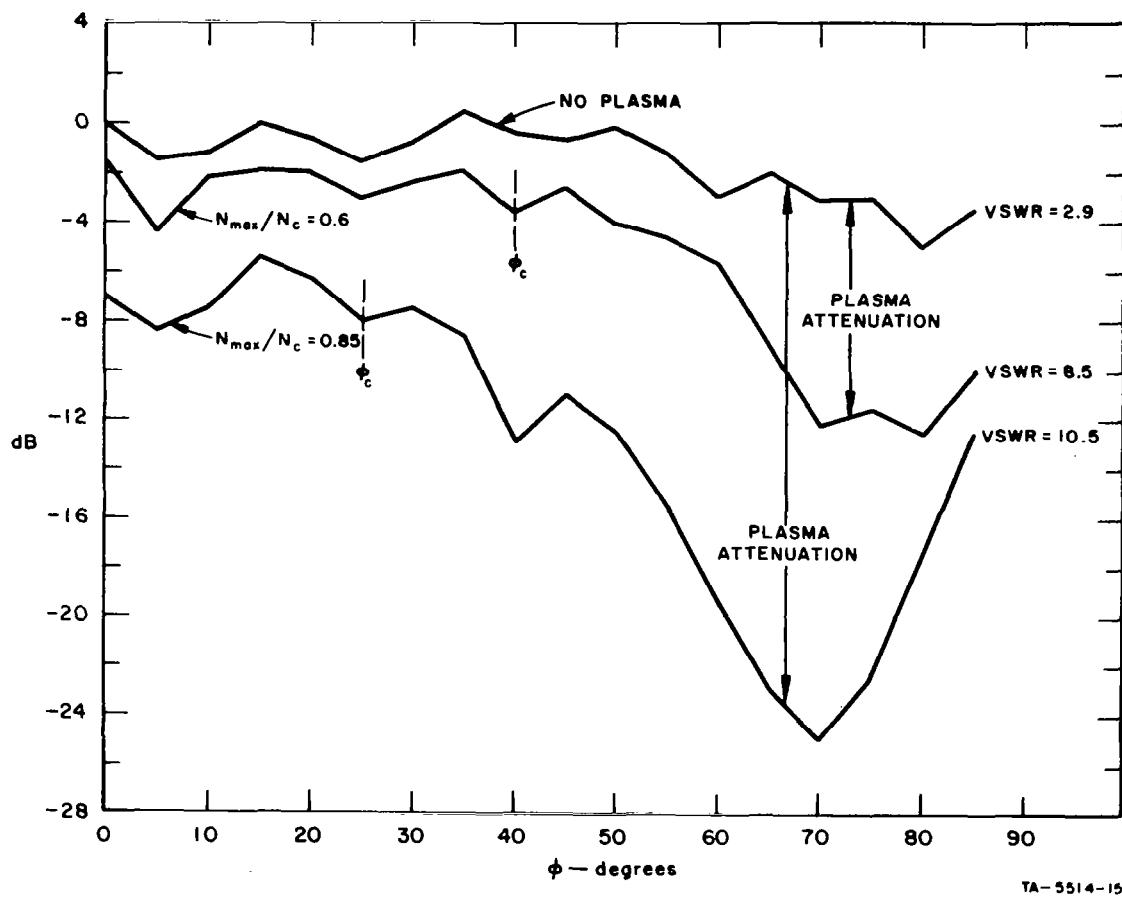
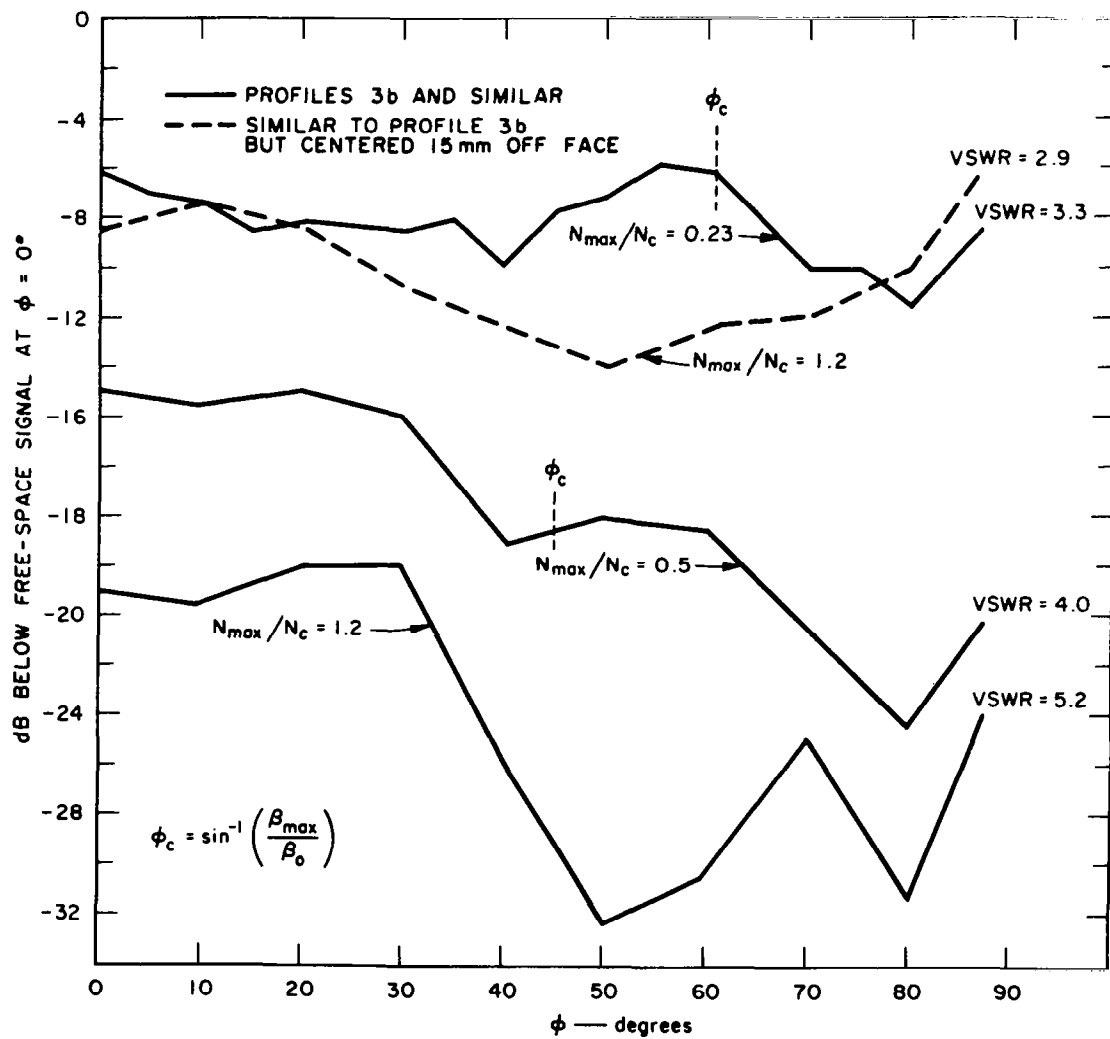


FIG. 15 PATTERNS OF TEFLON-FILLED SLOT COMPARED WITH FREE SPACE
(Profiles Similar to 2a)



TB-5514-16

FIG. 16 PATTERNS OF TEFLON SLOT

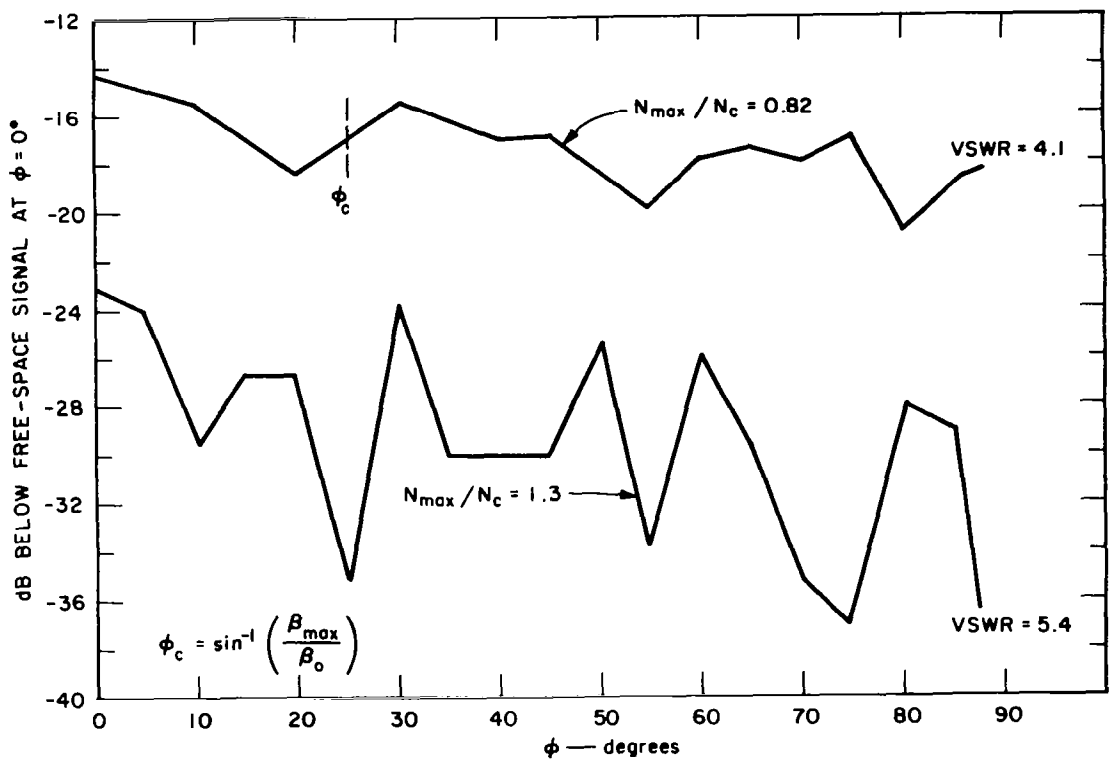


FIG. 17 PATTERNS MADE WITH THICKEST ELECTRON DENSITY PROFILES

line, the tube was against the antenna face, but for the dashed pattern, it was moved out until the VSWR was unaffected by the plasma -- about 1.5 cm away. Since the plane-wave losses in traversing such a plasma (at normal incidence) are calculated to be no greater than about 10 dB, the difference between the two patterns is interpreted as a demonstration of the loss in (far-field) transmission efficiency due to the plasma in the near field. Several such transmission measurements were made with the receiving horn fixed at $\phi = 0^\circ$, using both the Teflon and BN antennas confronted by thinner plasma profiles than used for the Fig. 16 patterns. The results of these measurements are shown in Fig. 18. Also shown as a function of $(\omega_p/\omega)^2$ are predicted plane-wave losses, calculated on the basis of profile 2b of Fig. 7. It is felt that the near agreement between this calculation and the measured losses with remote plasma is a measure of the accuracy of the ion probe diagnostics when profiles are measured.

The difference between attenuation for the two antennas with the close profile is attributable to the greater susceptibility of the Teflon antenna to plasma effects because of its higher near-field levels in free space. Figure 19 is a plot of signal received by a 5-mm long dipole used to probe the fields of the three antennas used in the measurements. Equal power was delivered to the antennas. The two dielectric-filled antennas follow approximately the rule-of-thumb that the signal falls by 10 dB one E-plane aperture dimension away from the face.

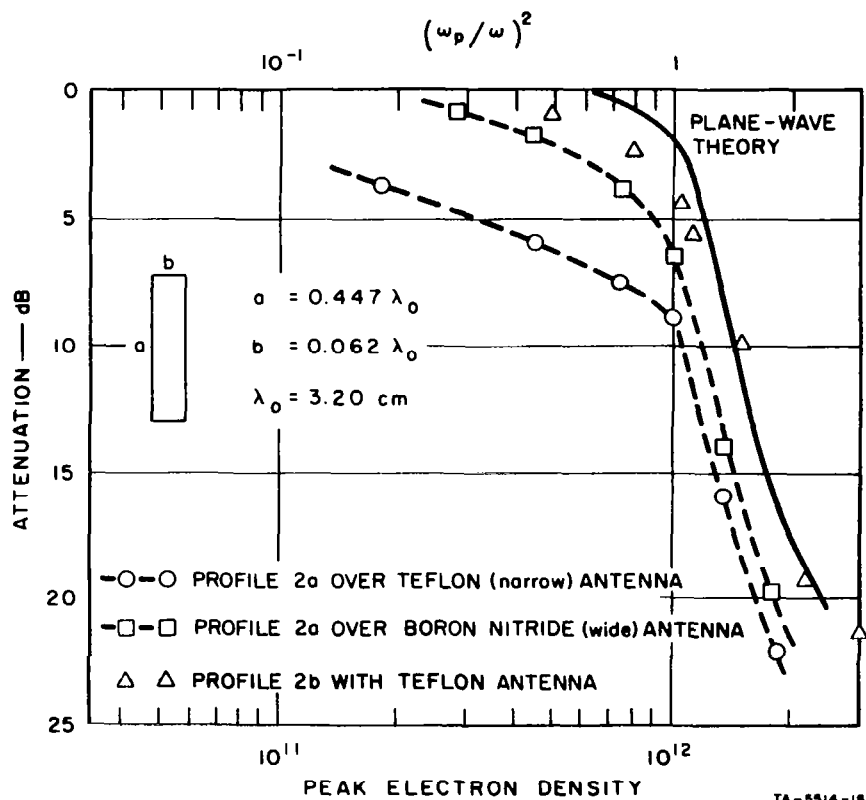


FIG. 18 MEASURED BROADSIDE ATTENUATION COMPARED WITH PLANE-WAVE THEORY

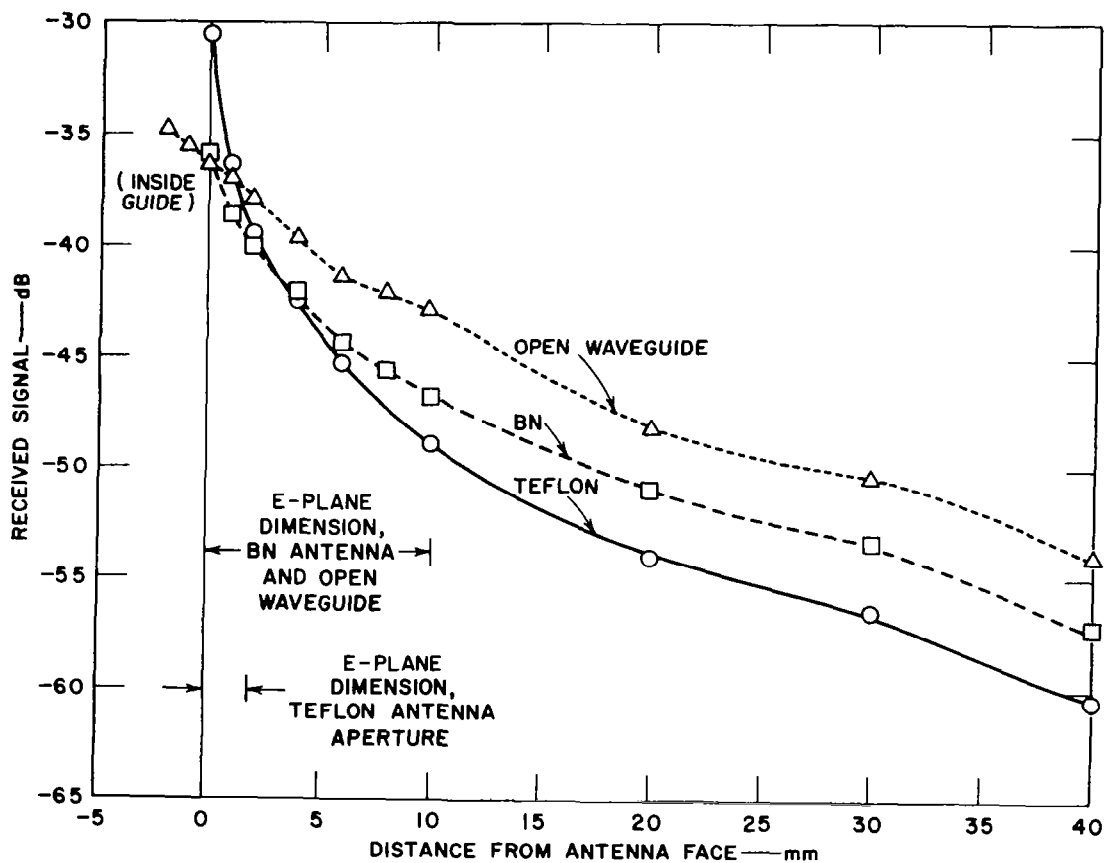


FIG. 19 PLOT OF SIGNAL RECEIVED BY 5-mm DIPOLE PROBE VERSUS DISTANCE ON AXIS

VI CONCLUSIONS AND RECOMMENDATIONS FOR FUTURE WORK

The measurements of impedance, transmission efficiency, and patterns show that efforts should be made in practice to exclude plasmas from the near fields of high performance transmitting antennas. On the other hand, if diagnostics of a plasma are desired, the reflection coefficient measurements have shown that the greater sensitivity can be achieved by maximum "filling" of the near-field region. Because of the demonstrated effects of a small nonuniform boundary layer, it is necessary to develop suitable analytical models before the potential accuracy of electron density diagnostics by this technique can be thoroughly evaluated. Without such models, the best generalization from the reflection coefficient data concerns the steep slope of $|\Gamma|$ vs $(\omega_p/\omega)^2$ rather than the absolute value of $|\Gamma|$. The steep slope appears to determine the electron density within a factor of about two for these low collision frequency plasmas. In the open waveguide measurements, it always occurred between $(\omega_p/\omega)^2 = 1.0$ and 2.0 , while with the two dielectric-filled slots it always occurred in the region $0.25 \lesssim (\omega_p/\omega)^2 \lesssim 0.5$.

As a result of these tests to date, it is important to compare reflection coefficient measurement with transmission (attenuation) measurement as diagnostic tools for flight tests:

- (1) Both measurements are useful over a limited range of electron density around the critical level.
- (2) Collision frequencies higher than ω may extend this range of electron density somewhat, but accuracy may suffer.
- (3) Since transmission also integrates over nonuniformities, the accuracy depends on knowledge of the profile.
- (4) If the plasma cannot be excluded from the near fields of the transmitting antenna, the several effects discussed in this report (mismatch, pattern changes, transmission efficiency) must be taken into account.
- (5) The transmission measurement will usually be preferable above critical (until dynamic range is exceeded) because the reflection coefficient is quite flat there.

- (6) Because of pattern effects, transmission between vehicle and ground is subject to important errors in knowledge of vehicle orientation that do not affect the reflection measurement.

It is concluded that either technique presently leaves much to be desired as a general tool in flight test diagnostics.

It is noteworthy that the greatest success in achieving agreement between plasma theory and laboratory measurements of the kind reported here has been found by those investigators who used either scaled dielectrics¹⁰ or wire grids¹¹ instead of plasma in their experiments. Prominent by their absence in such experiments are (1) nonuniformities in the near field and (2) extraneous plasma containers. In the impedance tests reported here, the containers were of minor importance because the entire experiment was designed to be performed within the plasma container. However, since it is inevitable that plasmas will exhibit the boundary layer nonuniformities, it is very important to develop a more sophisticated theory to compare with these experiments.

More complete data appears necessary to complete a comprehensive study of these effects to accompany the theoretical developments.

Future tests should include:

- (1) total impedance measurements rather than reflection coefficient alone;
- (2) Measurements with antennas purposely tuned for low reflection coefficient in free space, thereby increasing the range of reflection coefficient available for plasma effects;
- (3) higher collision frequency measurements; and
- (4) use of antennas specifically designed for such tests or for re-entry vehicles.

REFERENCES

1. W. C. Taylor, "The Effects of a Plasma in the Near-Zone Field of an Antenna," Final Report, Contract NAS1-3099, SRI Project 4555, Stanford Research Institute, Menlo Park, California (June 1964)
2. J. C. Camm and P. H. Rose, "Electric Arc-Driven Shock Tube," Phys. Fluids 6, No. 5, pp. 663-678 (May 1963)
3. H. R. Bredfeldt, W. E. Scharfman, H. Guthart, T. Morita, "The Use of Ion Probes in Re-Entry Physics," Tech. Report 26, Contract SD-103 under ARPA Order 281-62, SRI Project 3857-5, Stanford Research Institute, Menlo Park, California (May 1965)
4. W. E. Scharfman, "The Use of Langmuir Probes to Determine the Electron Density Surrounding Re-Entry Vehicles," Final Report, Contract NAS1-3942, SRI Project 5034, Stanford Research Institute, Menlo Park, California (June 1965)
5. H. R. Bredfeldt, W. E. Scharfman, H. Guthart, T. Morita, "Boundary Layer Ion Density Profiles as Measured by Electrostatic Probes," Tech. Report 33, Contract SD-103 under ARPA Order 281-62, SRI Project 3857-5, Stanford Research Institute, Menlo Park, California (February 1966)
6. G. Hok, et al., "Dynamic Probe Measurements in the Ionosphere," Scientific Report FS-3, University of Michigan Research Institute, Reprinted under Contract AF 19(604)-1843 (November 1958)
7. W. E. Scharfman, "The Use of Langmuir Probes to Determine the Electron Density Surrounding Re-Entry Vehicles," Final Report, Contract NAS1-2967, SRI Project 4556, Stanford Research Institute, Menlo Park, California (January 1964)
8. R. T. Compton, Jr., "The Admittance of Aperture Antennas Radiating into Lossy Media," Report 1691-5, Grant Number NsG-448, Ohio State University Research Foundation, Columbus, Ohio (March 1964)
9. G. Meltz, P. J. Freyheit, and C. Lustig, "The Admittance of a Plasma-Covered Cylindrical Antenna," RR-65-92, Sperry Rand Research Center, Sudbury, Massachusetts (September 1965)

10. G. Tyras, P. C. Bargeliotes, J. M. Hamm, R. R. Schell, "An Experimental Study of Plasma Sheath Effects on Antennas," Scientific Report No. 1, Contract No. AF 19(628)-3834, The University of Arizona Engineering Research Laboratories, Tucson, Arizona (December 1964)
11. T. M. Smith and K. E. Golden, "Radiation Patterns for a Slotted Cylinder Surrounded by a Plasma Sheath," IEEE Trans. Ant. and Prop. AP-13, 5, pp.775-780 (September 1965)